Investigation of defect levels in $BaSi_2$ epitaxial films by photoluminescence and the effect of atomic hydrogen passivation

To cite this article: Louise Benincasa *et al* 2019 *J. Phys. Commun.* **3** 075005

Journal of Physics Communications

PAPER

Investigation of defect levels in $BaSi_2$ epitaxial films by photoluminescence and the effect of atomic hydrogen passivation

Louise Benincasa[1,2], **Hirofumi Hoshida**[3], **Tianguo Deng**[1], **Takuma Sato**[1,2], **Zhihao Xu**[1], **Kaoru Toko**[1], **Yoshikazu Terai**[3] **and Takashi Suemasu**[1]

[1] Institute of Applied Physics, University of Tsukuba, Tsukuba, Ibaraki 305-8573, Japan
[2] Materials Department, University of Grenoble-Alpes, 38400 Saint-Martin-d'Hères, France
[3] Department of Computer Science and Electronics, Kyushu Institute of Technology, Iizuka, Fukuoka 820-8502, Japan

Keywords: photoluminescence, solar cell, defect, $BaSi_2$, interface

OPEN ACCESS

RECEIVED
12 June 2019

ACCEPTED FOR PUBLICATION
5 July 2019

PUBLISHED
18 July 2019

Abstract

Photoluminescence (PL) measurements were carried out on 0.5-μm thick $BaSi_2$ epitaxial films grown on Si(111) substrates with various Ba-to-Si deposition rate ratios (R_{Ba}/R_{Si}) in the range of 1.7–5.1. The samples were excited from both the frontside ($BaSi_2$) and the backside (Si substrate), at temperatures in the range of 8–50 K. These measurements have highlighted the existence of localized states within the bandgap that result from defects in the $BaSi_2$ films. The PL intensity is highly dependent on the excitation power, temperature, and R_{Ba}/R_{Si}. Of those studied, the $BaSi_2$ film at $R_{Ba}/R_{Si} = 4.0$ showed the most intense PL and weak photoresponsivity, whereas the PL intensity was weaker for the other samples. Therefore, we chose this sample for a detailed PL investigation. Based on the results we determined the energy separation between localized states, corresponding to PL peak energies. The difference in PL spectra excited from the $BaSi_2$-side and Si-side is attributed to the difference in kinds of defects emitting PL. The photoresponsivity of the $BaSi_2$ was drastically enhanced by atomic hydrogen passivation, and the PL intensity of the sample decreased accordingly.

1. Introduction

Si thin film solar cells have been studied extensively in the past decade [1–6]; however, with this material it is not easy to attain a high efficiency (η), such as at the level of 20%. Thus, many researchers have been working on Cu(In,Ga)(S,Se)$_2$, CdTe, and perovskite solar cells to drive improvements in η at lower cost. However, these materials contain nonabundant and/or toxic elements [7–11]. Thus, exploring alternative materials for thin film solar cells is very important. We have paid considerable attention to barium disilicide ($BaSi_2$), which is a new alternative for next generation solar cell applications [12]. The unit cell of $BaSi_2$, shown in figure 1, contains eight barium atoms (Ba) and 16 silicon atoms (Si). $BaSi_2$ is composed of abundant elements and it can be grown epitaxially on both Si(111) and Si(001) substrates with its *a*-axis normal to the substrate surface [13]. It has many attractive features, making it a good candidate for solar cell applications, such as those requiring a suitable bandgap of 1.3 eV; a large optical absorption coefficient of 3×10^4 cm^{-1} for a photon energy of 1.5 eV, which is more than 40 times higher than that of crystalline Si [14–17]; a long minority carrier lifetime of about 10 μs [18–20]; and a large minority carrier diffusion length of about 10 μm [21]. Recently, with the help of a-Si passivation layers, we achieved an η approaching 10% in p-$BaSi_2$/n-Si heterojunction solar cells [22, 23], and demonstrated the operation of $BaSi_2$ homojunction solar cells [24]. To further improve the η of $BaSi_2$ solar cells, it is important to fabricate high-quality $BaSi_2$ epitaxial films. Deep level transient spectroscopy (DLTS) revealed that undoped-$BaSi_2$ films contain electrically active defect levels [25, 26]. DLTS is, however, available only to defects in a depletion region. We, therefore, need to form a junction to expand the depletion region towards the region where defects exist. In contrast to DLTS, there is no such restrictions in photoluminescence (PL). Many studies have been carried out on the defects characterization of crystalline Si using PL [27–32]. However, to the best of our knowledge, there has been only one report on the PL of $BaSi_2$ bulk [33]. The goal of the present study is to evaluate the defects properties, such as the energy levels in $BaSi_2$ films. Previous research shows that the Ba-to-Si deposition rate ratio (R_{Ba}/R_{Si}) during molecular beam epitaxy (MBE) has an enormous impact on carrier

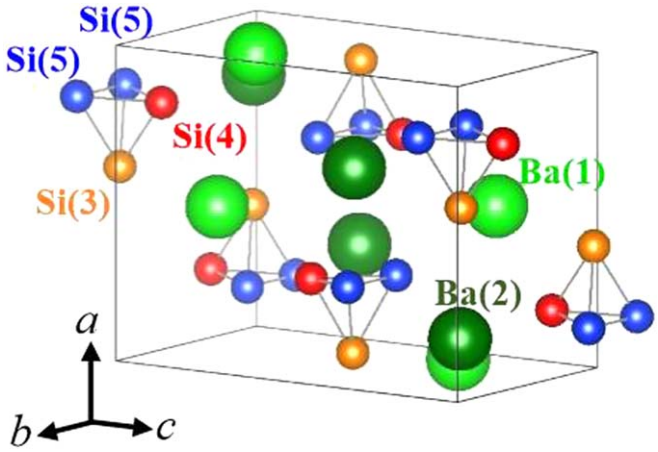

Figure 1. Crystal structure of $BaSi_2$.

concentration and photoresponsivity of $BaSi_2$ [34]. We therefore decided to analyze $BaSi_2$ films grown with different values of R_{Ba}/R_{Si} by PL. We also investigate the effect of atomic hydrogen on the PL spectra of $BaSi_2$ films because it enhances markedly the photoresponsivity of the $BaSi_2$ films [35, 36]. In this way, we will be able to gain improved understanding of the origin of these defects and find a way to suppress or reduce them.

2. Experimental

The fabrication process for $BaSi_2$ thin film is as follows: First, a Czochralski (CZ) n- Si(111) substrate (resistivity $\rho < 0.01$ Ωcm) was cleaned by organic cleaning, which is the standard cleaning process to remove substances such as grease. Then, the Si substrate underwent thermal cleaning (TC) in an ultrahigh vacuum chamber maintained at 900 °C for 30 min. A 3-nm thick $BaSi_2$ template layer was then deposited by reactive deposition epitaxy [26], which is the deposition of Ba atoms on heated Si substrates under high vacuum, commonly 10^{-7} Pa at 500 °C. This layer works as a seed crystal to control the crystal orientation of $BaSi_2$ for subsequent fabrication. Then, Ba and Si atoms were simultaneously codeposited by MBE at 580 °C to form a 450-nm thick undoped-$BaSi_2$. An important parameter during MBE growth is R_{Ba}/R_{Si}, which has a significant effect on the performance of $BaSi_2$ solar cells and for which the photoresponsivity reaches a maximum at $R_{Ba}/R_{Si} = 2.2$ [34]. In this experiment, we varied the R_{Ba}/R_{Si} from 1.7 to 5.1. Finally, a 3-nm thick a-Si layer was deposited on the $BaSi_2$ thin film at 180 °C. The a-Si capping layer suppresses the surface oxidation and behaves as a surface passivation layer [35]. For another sample, we supplied atomic H produced by a radiofrequency plasma gun for 15 min to a 0.5-μm thick $BaSi_2$ epitaxial layer ($R_{Ba}/R_{Si} = 2.2$) at 580 °C, followed by capping with a 3-nm thick a-Si layer deposited at 180 °C [35]. 80-nm thick indium-tin-oxide (ITO) electrodes of 1 mm in diameter were sputtered on the front surface and 150-nm thick Al electrodes were put on the back surface of the Si substrate for the photoresponse measurements.

Sample preparation details are summarized in table 1.

Photoresponse spectra were measured at RT using a lock-in technique with a xenon lamp and a 25 cm focal length single monochromator (Bunko Keiki SM-1700A and RU-60N). The light intensity was calibrated using a pyroelectric sensor (Melles Griot 13PEM001/J). PL measurements were carried out at various temperatures ranging from 8 to 50 K by exciting the samples from the $BaSi_2$ side and the Si side. The excitation wavelength was 442 or 552 nm. The PL was analyzed by a 25 cm focal length single monochromator, detected by a liquid nitrogen cooled Ge pin (Applied Detector 403L) or InP/InGaAs photomultiplier (PMT) (Hamamatsu Photonics R5509-72) and amplified by the lock-in technique. In the Si-side excitation, the laser line was introduced from the Si substrate; photoexcited carriers were generated there and were transferred to the $BaSi_2$/Si interface, and the PL was detected from the $BaSi_2$ side. The depth profile of H atoms in 0.3-μm thick $BaSi_2$ epitaxial layers ($R_{Ba}/R_{Si} = 2.2$) was evaluated by secondary ion mass spectrometry (SIMS) using 5.0 kV C_s^+ primary ions.

3. Results and discussion

Figure 2(a) shows the relationship between R_{Ba}/R_{Si} and carrier concentration as evaluated by Hall measurements on $BaSi_2$ films grown on high-resistivity floating-zone Si(111) substrates (resistivity $>10^3$ Ωcm)

Table 1. Sample preparation: $BaSi_2$ layer thickness (d), R_{Ba}/R_{Si}, and atomic hydrogen supply duration (t_H).

Sample	d (μm)	R_{Ba}/R_{Si}	t_H (min)
A	0.5	1.7	0
B	0.5	2.0	0
C	0.5	2.2	0
D	0.5	3.1	0
E	0.5	4.0	0
F	0.5	5.1	0
G	0.5	2.2	15
H	0.3	2.2	15
I	0.3	2.2	0

[34]. In a previous work, it was found that the carrier type of the $BaSi_2$ films grown with $R_{Ba}/R_{Si} = 2.0$ and 2.2 was p-type, and that the hole concentration of $BaSi_2$ films with $R_{Ba}/R_{Si} = 2.2$ reached a minimum of approximately 1×10^{15} cm^{-3} [34]. Furthermore, other samples showed n-type conductivity, and the electron concentration increases for both increasing and decreasing R_{Ba}/R_{Si} values. The electron concentration of $BaSi_2$ films with $R_{Ba}/R_{Si} = 4.0$ was approximately 7×10^{17} cm^{-3}. According to first-principles calculation by Kumar *et al* [37] Si vacancy (V_{Si}) is most likely to exist among point defects in $BaSi_2$, giving rise to localized states within the bandgap. Thus, it is considered that $BaSi_2$ films in sample E ($R_{Ba}/R_{Si} = {}^{4}.0$) would contain many V_{Si} because it was grown under Si poor conditions.

Photoresponse spectra were measured for samples A–F with different R_{Ba}/R_{Si} ranging from 1.7 to 5.1. A bias voltage (V_{bias}) of -1 V was applied to the front ITO electrode with respect to the backside Al electrode, with results presented in figure 2(b) [34]. Samples B ($R_{Ba}/R_{Si} = 2.0$) and C ($R_{Ba}/R_{Si} = 2.2$), they being in the vicinity of stoichiometry, present the most intense photoresponsivity. The photoresponsivity increases sharply for photon energies higher than the bandgap of $BaSi_2$. Low photoresponsivity means that photoexcited carriers recombine before they reach the electrodes. Therefore, it is reasonable to consider that all of the samples, except 2.0 and 2.2, contain more defects. Figure 2(c) shows the PL spectra of samples A–F measured at 9 K by the $BaSi_2$-side excitation using a 532 nm laser. The PL intensity differs depending on R_{Ba}/R_{Si}. Sample E ($R_{Ba}/R_{Si} = 4.0$) shows the most intense PL peak, while the PL intensity is weaker for the other samples. $BaSi_2$ is an indirect bandgap semiconductor; therefore, intense PL is obtained only when the localized states are generated. With an increase in R_{Ba}/R_{Si} from 2.2 to 4.0, the PL increases, meaning that the localized states are formed. However, any further increase in R_{Ba}/R_{Si} degrades the crystalline quality too much, and therefore PL could not be obtained for sample F ($R_{Ba}/R_{Si} = 5.1$). On the basis of these PL results, we chose sample E ($R_{Ba}/R_{Si} = 4.0$) to perform a detailed PL investigation for detecting localized states within the bandgap. Please note that DLTS measurement is difficult to perform for sample E because the electron concentration of the $BaSi_2$ films is close to 10^{18} cm^{-3} as shown in figure 2(a), and thus it is difficult to expand the depletion region towards the $BaSi_2$ films to evaluate defect levels there.

The PL intensity against the excitation power (P) for sample E at 9 K is shown in figure 3. The inset shows the PL spectrum at $P = 240$ mW cm^{-2}, measured at 9 K. The PL spectrum was well reproduced by four Gaussian curves as denoted by peaks 1–4 at 0.86, 0.98, 1.04, and 1.12 eV, respectively. For the low excitation range up to around $P = 10$ mW cm^{-2}, the PL intensity increases almost proportionally with P. The proportionality factor, γ, for each spectrum is close to 1. However, for the higher excitation range, γ becomes much smaller than 1. This result suggests that the PL can be ascribed to the transition of electrons between localized states within the bandgap. In the low excitation range, as the excitation power increases, the number of electrons at higher localized states increases, leading to an increase in PL intensity. However, for much higher excitation, such localized states saturate, and therefore the PL intensity also begins to saturate.

Before moving on to discussing the differences in PL spectra by $BaSi_2$-side excitation versus Si-side excitation, we refer to the band alignment of the $BaSi_2$/Si heterostructure in figure 4. Because of the small electron affinity of $BaSi_2$ (3.2 eV) [38], there are large conduction band and valence band offsets at the heterointerface. This means that the transfer of holes generated in $BaSi_2$ into Si by the $BaSi_2$-side excitation are blocked by a large valence band discontinuity, ΔE_V, at the heterointerface. Similarly, the transfer of electrons generated in Si into $BaSi_2$ by the Si-side excitation are blocked by a large conduction band discontinuity, ΔE_C. Figure 5 shows the temperature dependence of the PL spectra of $BaSi_2$ film with $R_{Ba}/R_{Si} = 4.0$ excited by a 442 nm laser for (a) $BaSi_2$-side excitations and (b) Si-side excitations. For the $BaSi_2$-side excitation, the most intense peak is at around 1.01 eV, and broad PL spectra consisting of several luminescence peaks are observed. The absorption coefficient, α, at this wavelength reaches 6×10^5 cm^{-1} in $BaSi_2$ [14], meaning that the

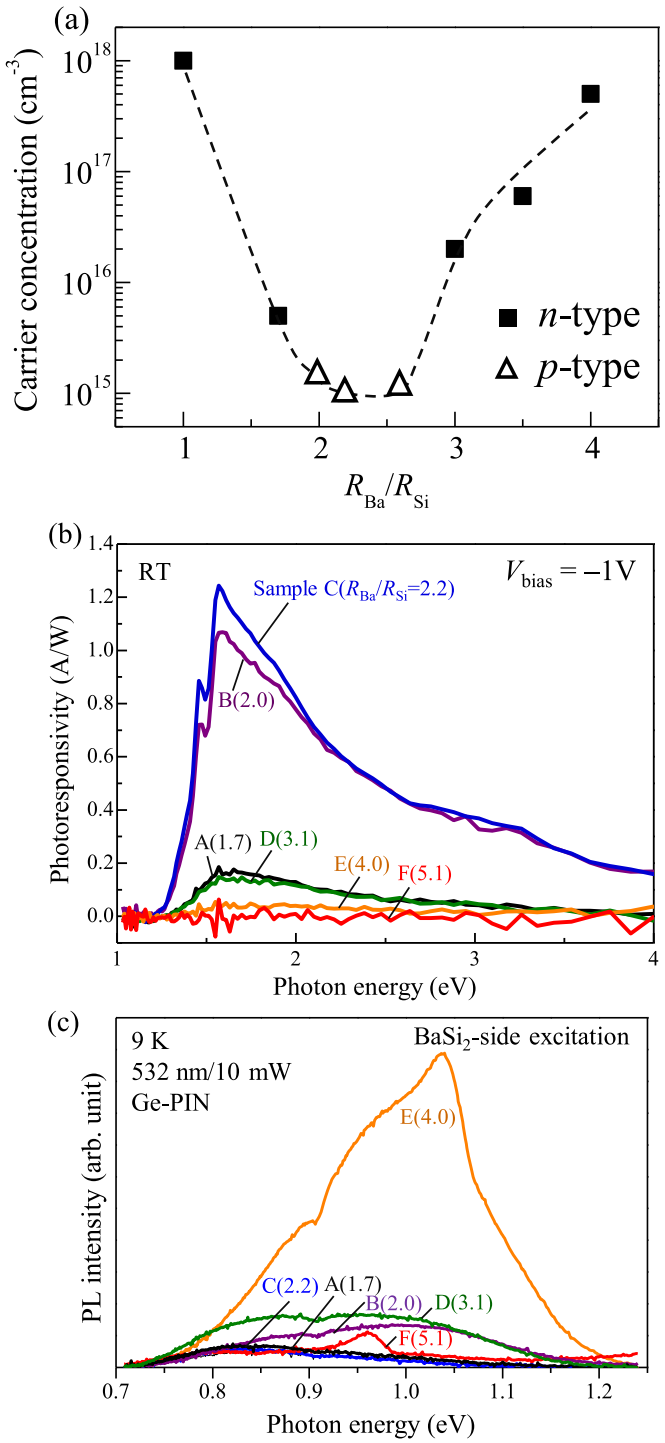

Figure 2. (a) Carrier concentration and (b) photoresponse spectra of samples A-F at RT [34] and (c) their PL spectra at 9 K for $BaSi_2$ films with various values of R_{Ba}/R_{Si}, excited from the $BaSi_2$ side.

penetration depth of the laser light is estimated to be $3/\alpha \sim 50$ nm. Therefore, in the case of $BaSi_2$-side excitation the photogenerated carriers (electron and holes) recombine within the $BaSi_2$ films. The PL intensity decreases with an increase in temperature because of the increase in the nonradiative recombination rates. On the other hand, for backside excitation we see several peaks, including one that is very sharp at around 0.76 eV. The quantum efficiency of the detector (InP/InGaAs PMT) is known to decrease significantly for wavelengths beyond 1.6 μm (<0.77 eV). To confirm the presence of the sharp PL peak at around 0.76 eV, we measured PL spectra using the Ge pin detector, which detects wavelengths well above 1.6 μm. We also measured the PL spectrum of sample B ($R_{Ba}/R_{Si} = 2.0$) for comparison. As shown in figure 5(c), the sharp PL surely exists, meaning that such sharp PL is attributed to defects around the $BaSi_2$/Si interface. This is because photogenerated electrons cannot be transferred into the $BaSi_2$ film because of the large ΔE_C as shown in figure 4.

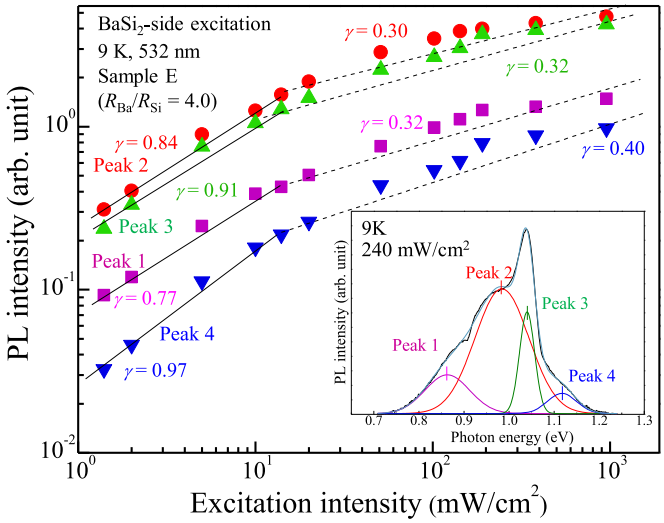

Figure 3. $BaSi_2$-side excitation power dependence of PL intensity for each peak for sample E ($R_{Ba}/R_{Si} = 4.0$) at 9 K.

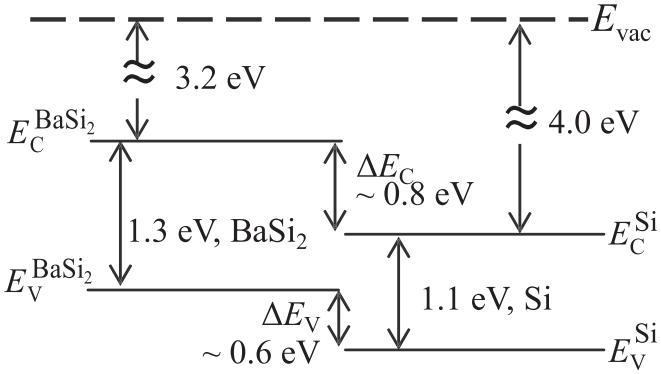

Figure 4. Band alignment of $BaSi_2$/Si.

Another sharp peak at around 1.08 eV was observed in figure 5(b), which is associated with the Si substrate. Compared to a significant difference in PL spectra between samples B and E when excited by the $BaSi_2$ side in figure 2(c), there is not much difference in their PL spectra in figure 5(c), which were obtained by the Si-side excitation. These results indicate that the defects properties around the $BaSi_2$/Si interface such as defect levels and their densities are almost the same in $BaSi_2$ films regardless of the R_{Ba}/R_{Si}.

To have an in-depth understanding of localized states, we analyze the PL properties in more detail using figures 6 and 7. First, figure 6(a) shows the Gaussian fitting curves to reproduce the PL spectrum of sample E, $BaSi_2$ films with $R_{Ba}/R_{Si} = 4.0$, by the $BaSi_2$-side excitation at 8 K. The excitation power was 60 mW cm^{-2}. The spectrum is composed of three integrated peaks at 0.943 eV (peak F1), 1.016 eV (peak F2), and 1.111 eV (peak F3), all of which have different origins. The photon energy associated with the PL peak corresponds to the energy separation between two localized states within the bandgap of the $BaSi_2$. According to the DLTS measurement on $BaSi_2$ epitaxial films [26], a hole trap level, caused by V_{Si}, is located approximately 0.27 eV above the valence band maximum (VBM). Therefore, we speculate that PL peaks F1 and F2 in figure 6(a) are related to transitions via this hole trap level in $BaSi_2$. Figure 6(b) shows the PL spectrum of the CZ-Si(111) substrate at 8 K, composed of a sharp and intense peak at around 1.08 eV (red), and two small peaks at around 1.04 eV (blue), and 1.12 eV (light blue) due to exciton-related luminescence [28]. In the case of Si-side excitation, in addition to the above three peaks originating from the Si substrate, three peaks at 0.761 eV (peak B1), 0.843 eV (peak B2), and 0.957 eV (peak B3) appear in figure 6(c). In our previous work [39], we found that an electron trap level located at 0.33 eV below the conduction band minimum (CBM) in the n-Si substrate near the $BaSi_2$/n-Si interface, which is caused by the TC at 900 °C for removal of oxide layers on the Si substrate. We also found that a hole trap level at 0.19 eV above the VBM of Si, caused by the diffusion of Ba into the n-Si substrate, and an electron trap level at 0.1 eV from the CBM of Si [40]. From the information obtained in this study, we are able to draw the diagram of a

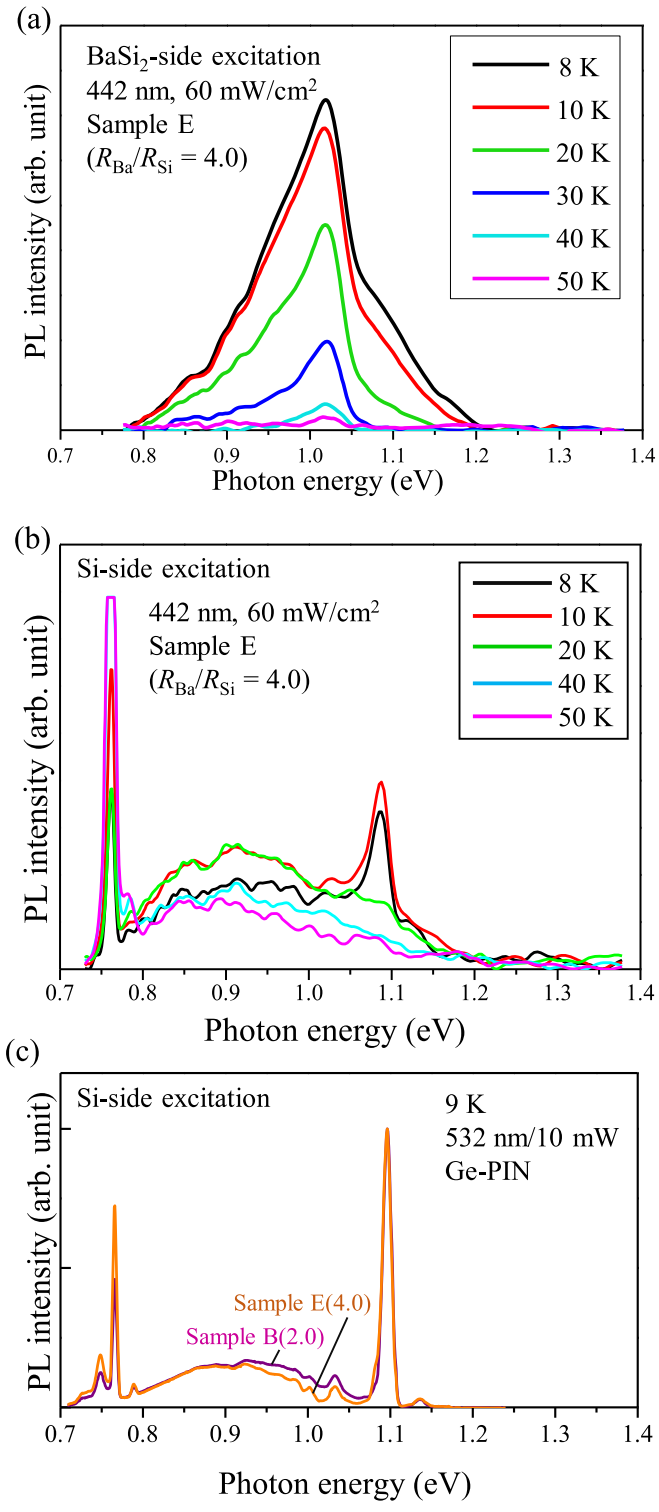

Figure 5. Temperature dependence of PL spectra of sample E, $BaSi_2$ film with $R_{Ba}/R_{Si} = 4.0$ for (a) $BaSi_2$-side excitation and. (b) Si-side excitation measured using the InP/InGaAs PMT. (c) PL spectra excited from the Si side for samples B and E using the Ge PIN detector at 9 K.

bandgap structure of sample E, as shown in figure 7. This figure shows the energy levels and the energy separation between two localized states within the bandgap in the $BaSi_2$. However, we do not know the precise location of these defect levels in the bandgap. More measurements, such as DLTS, would have to be performed to obtain more precise results about this study.

We next discuss the effect of atomic hydrogen supply on the PL and photoresponse spectra of $BaSi_2$ films. Figure 8(a) shows the photoresponse spectra of samples C ($R_{Ba}/R_{Si} = 2.2$ without atomic H) and G ($R_{Ba}/R_{Si} = 2.2$ with atomic H) at $V_{bias} = -0.3$ V at RT. To our surprise, by H passivation the photoresponsivity of sample G increased drastically by a factor of 6 compared with that of sample C, as shown in figure 8(a). The

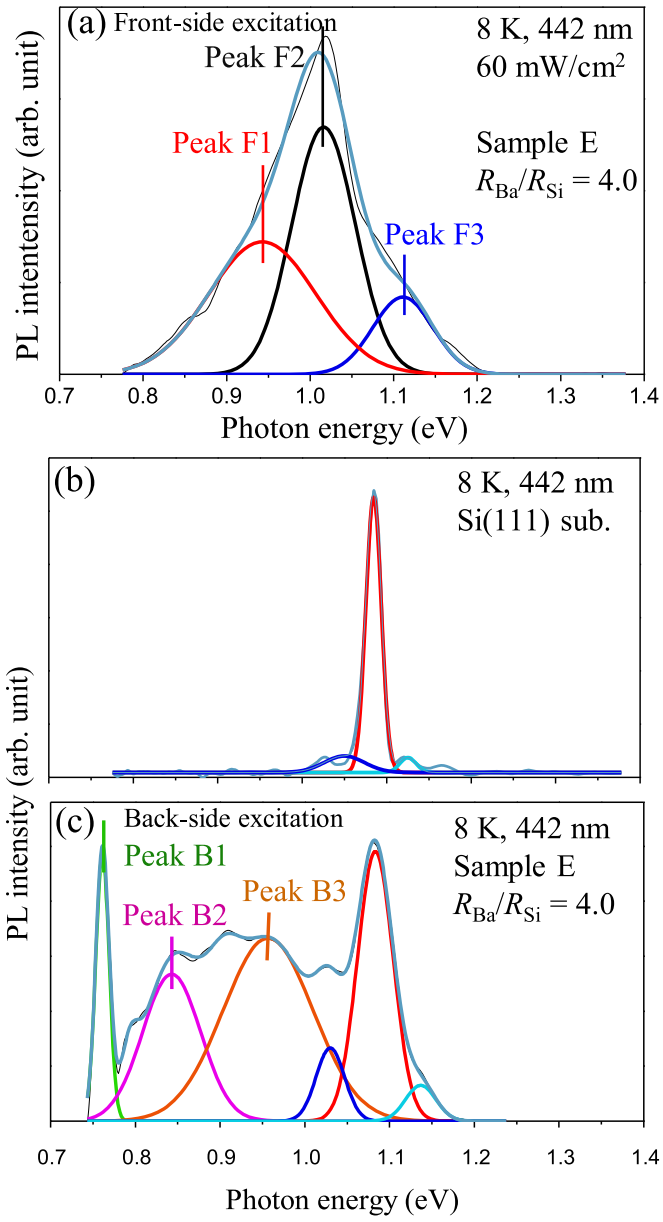

Figure 6. Gaussian fitting of PL spectra of sample E, $BaSi_2$ film with $R_{Ba}/R_{Si} = 4.0$, measured at 8 K for. (a) $BaSi_2$-side excitation and (c) Si-side excitation. (b) PL spectrum of CZ-Si(111) substrate at 8 K.

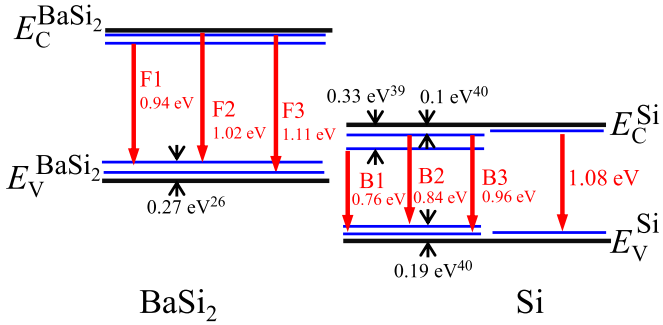

Figure 7. Defect levels observed in a bandgap structure of $BaSi_2$.

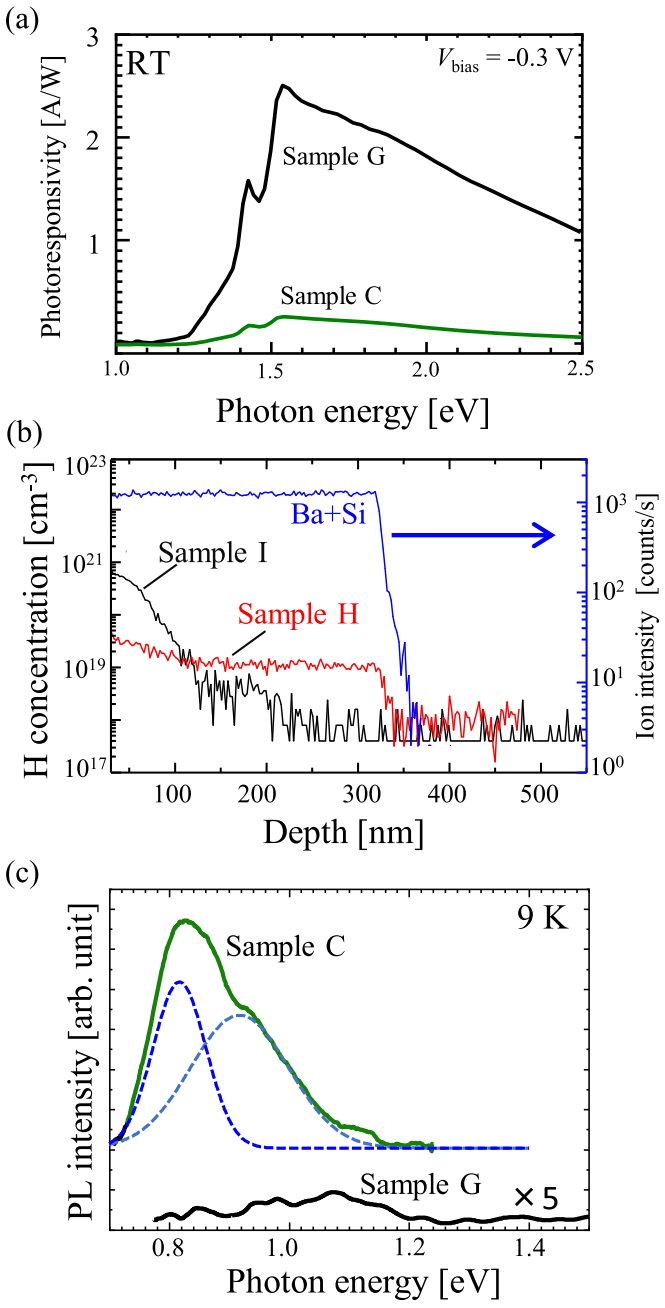

Figure 8. (a) PR spectra of samples C and G at RT, showing the significant improvement of photoresponsivity in sample G. (b) SIMS depth profiles of H atom and ions (Ba + Si) of $BaSi_2$ films in sample H. H depth profile in sample I is also shown for comparison. (c) PL spectra of samples C and G at 9 K. Sub-bandgap PL disappeared after the introduction of atomic H in sample G.

SIMS depth profiles of H and the secondary ion (Ba + Si) intensities in sample H, approximately 0.3-μm thick $BaSi_2$ films, are shown in figure 8(b). The concentration of H atoms reached about 1×10^{19} cm^{-3} at depths of 20–320 nm from the surface. This H concentration is higher than that of sample I without atomic H, in which the H atoms seem to diffuse from the surface into the deeper bulk region of $BaSi_2$. We cannot distinguish H from H_2 by SIMS. Thus, there is a possibility that H_2 molecules exist in sample I. This is because H_2 molecules are difficult to evacuate from the ion-pumped MBE chamber. We, therefore, consider that H_2 molecules might enter $BaSi_2$ films during sample fabrication. As shown in figure 8(c), the sub-bandgap PL decreased significantly in sample G, in accordance with the photoresponse enhancement, as shown in figure 8(a). The PL in $BaSi_2$ originates from the transition between localized states within the bandgap. Consequently, these results mean that the $BaSi_2$ active localized states in sample C are decreased by the H introduction in sample G, leading to the enhancement of photoresponsivity. Therefore, it is reasonable to consider that the defect levels in the $BaSi_2$ films become inactive by H treatment and that these defects are passivated by atomic H. On the basis of these results, we may reasonably conclude that PL is an effective means of understanding the presence of defects in $BaSi_2$.

4. Summary

We fabricated 0.5-μm thick undoped $BaSi_2$ epitaxial films on Si(111) substrates by MBE with various values of R_{Ba}/R_{Si} ranging from 1.7 to 5.1 and characterized them by PL measurement. Results have highlighted that the PL can be ascribed to the transition of electrons between the localized states within the bandgap, as a result of defects contained in the semiconductors. The PL is highly dependent on power excitation, temperature, and R_{Ba}/R_{Si}. Of all the films studied, the $BaSi_2$ film at $R_{Ba}/R_{Si} = 4.0$ showed the most intense PL intensity. From the results obtained on this sample, the energy between the localized states within the bandgap were obtained. Differences in PL spectra from $BaSi_2$-side and Si-side excitation are attributed to the different kinds of defects. The bandgap structure with various defect levels in $BaSi_2$ films with $R_{Ba}/R_{Si} = 4.0$ was also drawn. Finally, $BaSi_2$ films passivated with atomic H showed high photoresponsivity but the PL intensity was very weak. We, therefore, conclude that defects in the $BaSi_2$ structure become inactivated by atomic H, leading to the enhancement of photoresponsivity.

Acknowledgments

This work was financially supported by JSPS KAKENHI Grant Numbers 17K18865, 18H01477, and 18H03767 and JST MIRAI.

ORCID iDs

Takashi Suemasu https://orcid.org/0000-0001-6012-4986

References

[1] Sai H, Matsui T, Koida T, Matsubara K, Kondo M, Sugiyama S, Katayama H, Takeuchi Y and Yoshida I 2015 *Appl. Phys. Lett.* **106** 213902
[2] Trompoukis C *et al* 2015 *Phys. Stat. Solidi* A **1** 140
[3] Tan H, Moulin E, Si F T, Schüttauf J W, Stuckelberger M, Isabella O, Haug F J, Ballif C, Zeman M and Smets A H M 2015 *Prog. Photovolt: Res. Appl.* **23** 949
[4] Sai H, Matsui T, Saito K, Kondo M and Yoshida I 2015 *Prog. Photovolt: Res. Appl.* **23** 1572
[5] Meillaud F, Boccard M, Bugnon G, Despeisse M, Hänni S, Haug F-J, Persoz J, Schüttauf J-W, Stuckelberger M and Ballif C 2015 *Mater. Today* **18** 378
[6] Konagai M 2011 *Jpn. J. Appl. Phys.* **50** 030001
[7] Jackson P, Hariskos D, Wuerz R, Kiowski O, Bauer A, Friedlmeier T M and Powalla M 2015 *Phys. Stat. Solidi RRL* **9** 28
[8] Jackson P, Wuerz R, Hariskos D, Lotter E, Witte W and Powalla M 2016 *Phys. Stat. Solidi RRL* **10** 583
[9] Wu X 2004 *Sol. Energy* **77** 803
[10] Burschka J, Pellet N, Moon S-J, Humphry-Baker R, Gao P, Nazeeruddin M K and Grätzel1 M 2013 *Nature* **499** 316
[11] Yang W S, Noh J H, Jeon N J, Kim Y C, Ryu S, Seo J and Seok S I 2015 *Science* **348** 1234
[12] Suemasu T and Usami N 2017 *J. Phys.* D **50** 023001
[13] McKee R A, Walker F J, Conner J R and Raj R 1993 *Appl. Phys. Lett.* **63** 2818
[14] Toh K, Saito T and Suemasu T 2011 *Jpn. J. Appl. Phys.* **50** 068001
[15] Migas D B, Shaposhnikov V L and Borisenko V E 2007 *Phys. Status Solidi* B **244** 2611
[16] Kumar M, Umezawa N and Imai M 2014 *J. Appl. Phys.* **115** 203718
[17] Kumar M, Umezawa N and Imai M 2014 *Appl. Phys. Express* **7** 071203
[18] Hara K O, Usami N, Toh K, Baba M, Toko K and Suemasu T 2012 *J. Appl. Phys.* **112** 083108
[19] Hara K O, Usami N, Nakamura K, Takabe R, Baba M, Toko K and Suemasu T 2013 *Appl. Phys. Express* **6** 112302
[20] Takabe R, Hara K O, Baba M, Du W, Shimada N, Toko K, Usami N and Suemasu T 2014 *J. Appl. Phys.* **115** 193510
[21] Baba M, Toh K, Toko K, Saito N, Yoshizawa N, Jiptner K, Sakiguchi T, Hara K O, Usami N and Suemasu T 2012 *J. Cryst. Growth* **348** 75
[22] Yachi S, Takabe R, Toko K and Suemasu T 2016 *Appl. Phys. Lett.* **109** 072103
[23] Deng T, Sato T, Xu Z, Takabe R, Yachi S, Yamashita Y, Toko K and Suemasu T 2018 *Appl. Phys. Express* **11** 062301
[24] Kodama K, Yamashita Y, Toko K and Suemasu T 2019 *Appl. Phys. Express* **12** 041005
[25] Takeuchi H, Du W, Baba M, Takabe R, Toko K and Suemasu T 2015 *Jpn. J. Appl. Phys.* **54** 07JE01
[26] Yamashita Y, Sato T, Toko K and Suemasu T 2018 *Jpn. J. Appl. Phys.* **57** 075801
[27] Drozdov N A, Patrin A A and Tkachev V D 1976 *Sov. Phys. JETP* **23** 597
[28] Suezawa B, Sasaki Y and Sumio K 1983 *Phys. Status Solidi* A **79** 173
[29] Sauer R, Weber J, Stolz J, Weber E, Kusters K and Alexander H 1985 *Appl. Phys. A: Solids Surf.* **36** 1
[30] Tajima M 1990 *J. Cryst. Growth* **103** 1
[31] Lightowlers E C and Higgs V 1993 *Phys. Status Solidi* A **138** 665
[32] Tajima M, Iwata Y, Okayama F, Toyota H, Onodera H and Sekiguchi T 2012 *J. Appl. Phys.* **111** 113523
[33] Kishino S, Imai T, Iida T, Nakaishi Y, Shinada M, Takanashi Y and Hamada N 2007 *J. Alloy and Compd.* **428** 22
[34] Takabe R, Deng T, Kodama K, Yamashita Y, Sato T, Toko K and Suemasu T 2018 *J. Appl. Phys.* **123** 045703
[35] Xu Z, Gotoh K, Deng T, Sato T, Takabe R, Toko K, Usami N and Suemasu T 2018 *AIP Adv.* **8** 055306
[36] Xu Z *et al* 2019 *Phys. Rev. Mater* **3** 065403
[37] Kumar M, Umezawa N, Zhou W and Imai M 2017 *J. Mater. Chem.* A **5** 25293
[38] Suemasu T, Morita K, Kobayashi M, Saida M and Sasaki M 2006 *Jpn. J. Appl. Phys.* **45** L519

[39] Yamashita Y, Sato T, Bayu M E, Toko K and Suemasu T 2018 *Jpn. J. Appl. Phys.* **57** 075801
[40] Yachi S, Takabe R, Deng T, Toko K and Suemasu T 2018 *Jpn. J. Appl. Phys.* **57** 042301 8